

tation mechanism via inner-shell vacancies for the Pb + Pb and Pb + U systems. These calculations and the extrapolation for the U + U system, which does not include effects from the spreading of the  $1s\sigma$  state in the negative-energy continuum, reproduce the absolute positron yield as well as its dependence on  $Z$  and on the distances of closest approach within the limits of error.

We would like to acknowledge the achievements of the UNILAC crew in making excellent U beams, P. Maier-Komor and E. Kellner for fabricating the delicate U targets, M. Richter, R. Hadsell, and F. Weik for their computational assistance, and H. Stettmeier and L. Richter for helping us during the initial phase of the work. We thank W. Greiner, D. H. Jakubassa, M. Kleber, V. Oberacker, J. Reinhardt, H. Schmidt, G. Soff, and G. Süssmann for theoretical discussions and encouragement. This work was supported by grants of the Bundesministerium für Forschung and Technologie and in part by the Alexander von Humboldt-Stiftung. One of us (J.S.G.) acknowledges receipt of a Senior U. S. Scientist Award from the Alexander von Humboldt-Stiftung.

<sup>(a)</sup>On leave from Yale University, New Haven, Conn. 06520.

<sup>(b)</sup>Present address: Institut for Chemical Research, Kyoto University, Kyoto, Japan.

<sup>1</sup>H. Backe, E. Berdermann, H. Bokemeyer, J. S. Greenberg, L. Handschug, F. Hessberger, P. Kienle, C. Kozhuharov, Y. Nakayama, L. Richter, H. Stettmeier, P. Vincent, F. Weik, and R. Willwater, *J. Phys.*

*Soc. Jpn., Suppl.* **44**, 832 (1978).

<sup>2</sup>H. Backe, L. Handschug, F. Hessberger, E. Kankeleit, L. Richter, F. Weik, R. Willwater, H. Bokemeyer, P. Vincent, Y. Nakayama, and J. S. Greenberg, *Phys. Rev. Lett.* **40**, 1443 (1978).

<sup>3</sup>V. V. Voronkov and N. N. Kolesnikow, *Zh. Eksp. Teor. Fiz.* **39**, 189 (1961) [*Sov. Phys. JETP* **12**, 136 (1961)]; F. Beck, H. Steinwedel, and G. Süssmann, *Z. Phys.* **171**, 189 (1963); W. Pieper and W. Greiner, *Z. Phys.* **218**, 327 (1969); D. Rein, *Z. Phys.* **221**, 423 (1969).

<sup>4</sup>B. Müller, J. Rafelski, and W. Greiner, *Z. Phys.* **257**, 62, 183 (1972); Ya. B. Zel'dovich and V. S. Popov, *Usp. Fiz. Nauk* **105**, 403 (1972) [*Sov. Phys. Uspekhi* **14**, 673 (1972)].

<sup>5</sup>G. Soff, J. Reinhardt, B. Müller, and W. Greiner, *Phys. Rev. Lett.* **38**, 592 (1977).

<sup>6</sup>K. Smith, H. Peitz, B. Müller, and W. Greiner, *Phys. Rev. Lett.* **32**, 554 (1974).

<sup>7</sup>D. H. Jakubassa and M. Kleber, *Z. Phys. A* **227**, 41 (1976).

<sup>8</sup>E. Moll and E. Kankeleit, *Nukleonik* **7**, 180 (1965).

<sup>9</sup>W. E. Meyerhof, R. Anholt, Y. El Masri, I. Y. Lee, D. Cline, F. S. Stephens, and R. M. Diamond, *Phys. Lett.* **69B**, 41 (1977).

<sup>10</sup>D. H. Jakubassa, *Phys. Lett.* **58A**, 163 (1976).

<sup>11</sup>H. H. Behnke, P. Armbruster, F. Folkmann, J. R. Mac Donald, and P. H. Mokler, in *Proceedings of the Tenth International Conference on the Physics of Electronic and Atomic Collisions, Paris, France, 1977, Abstracts*, edited by M. Barat and J. Reinhardt (Commissariat à l'Énergie Atomique, Paris, 1977); H. H. Behnke, D. Liesen, S. Hagmann, P. H. Mokler, and P. Armbruster, to be published.

<sup>12</sup>B. Müller, G. Soff, W. Greiner, and V. Ceausescu, *Z. Phys. A* **285**, 27 (1978).

<sup>13</sup>J. Reinhardt, V. Oberacker, B. Müller, W. Greiner, and G. Soff, *Phys. Lett.* **78B**, 183 (1978), and private communication.

## Observation of Scattering of Ion-Acoustic Cylindrical Solitons

Y. Nishida, T. Nagasawa,<sup>(a)</sup> and S. Kawamata

*Department of Electrical Engineering, Utsunomiya University, Utsunomiya 321-31, Japan*

(Received 10 October 1978)

A large-amplitude ion-acoustic cylindrical soliton launched in an axisymmetric cylindrical system collapses at the center of the cylinder. The highly nonlinear nature of the interaction is observed after the collapse, showing that many isolated pulses are emitted abruptly and propagate out without clear evolution of their wave forms.

The solitary wave is one of the most interesting phenomenon in nonlinear physics.<sup>1,2</sup> They are known to relate not only to large-amplitude dispersive waves<sup>2,3</sup> in plasmas, including laser- and/or microwave-plasma-interaction phenomena, but also to the waves of hydrodynamics or

even to the oscillations in a lattice of solids.<sup>4</sup> Here we focus our attention on the ion-acoustic solitons. It has been clarified that the solitons do not interact strongly, i.e., elasticity has been observed in the collision process. On this point, rather small-amplitude, one-dimensional solitons

have been investigated both theoretically,<sup>5,6</sup> including numerical simulation, and experimentally<sup>3,7</sup> on the multiple solitons and interactions between them. But recent theoretical considerations have pointed out some possibilities of the inelastic process in the collision of solitons,<sup>4,8</sup> although, to our knowledge, experimental verifications have not been done yet. Characteristics of two-dimensional cylindrical<sup>9-11</sup> and three-dimensional spherical<sup>12</sup> solitons have also been predicted theoretically and have been confirmed precisely in the experiment on the cylindrical solitons.<sup>13,14</sup>

In the present Letter, we wish to present experimental results on new scattering phenomena occurring in the collisions of large-amplitude cylindrical ion-acoustic solitons, which may show the existence of inelastic processes in the collision of solitons.

An experiment is performed in a DP-type<sup>3,13,14</sup> coaxial cylindrical system covered with many permanent magnets on the chamber wall. The system is explained in another publication, here we summarize the plasma parameters: electron density  $n \approx (5-10) \times 10^8 \text{ cm}^{-3}$ , electron temperature  $T_e \approx 2.0-3.6 \text{ eV}$ , and that of ion  $T_i < 0.4 \text{ eV}$  in Ar gas with pressure of  $(1.5-5.0) \times 10^{-4} \text{ Torr}$ . Ion-ion and ion-neutral collisions can be ignored, while electrons have been measured to be Boltzmann distribution because of many collisions with the wall sheath. A pulse is applied between two plasmas to excite solitons. A cylindrical probe (0.5 diam  $\times$  3 mm) biased to the electron saturation is movable axially and can be rotated across the plasma column center. The probe bias is selected carefully so that the sheath thickness does not affect the results.

A typical example of the excited wave is shown in Fig. 1 observed at the center. The applied wide pulse (top trace) evolves and breaks into three solitons (bottom trace) accompanying a precursor in front of the main large-amplitude

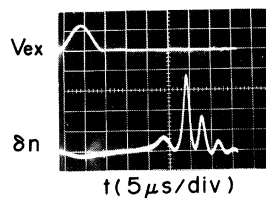


FIG. 1. Example of the applied pulse (top trace) and excited solitons observed at the column center (bottom trace).

wave.<sup>14</sup> The breaking into the completely separated multisolitons occurs abruptly in a very narrow region near the center, although overlapped multisolitons are observed until the pulse reaches the plasma center as observed by Hershkovitz, Romesser, and Montgomery.<sup>7</sup> In Fig. 2 are shown the spatial patterns of the soliton before and after the collision, i.e., the collapse at the center ( $t=0$ ). The first pulses, solitons, converge into ( $t < 0$ ) and collapse at the center ( $t=0$ ), then go through each other ( $t > 0$ ) like the one-dimensional case. Before the collapse, as mentioned above, there exist one or two small-amplitude solitons behind the large-amplitude pulse. However, they break into four pulses with almost the same amplitude after the collision. The completely different natures of the collision from the one-dimensional case<sup>3</sup> can be summarized as follows. First, the amplitude  $\delta n/n$  of the largest first pulse decreases rapidly as  $\delta n(r)/n \propto (r_0/r)^p$  with  $p \approx 1.0$  different from  $p \approx 0.5-0.6$  before the collapse.<sup>14</sup> Second, the solitons appear to break into or emit many isolated pulses having the velocity larger than before collapse, while the width,  $D$ , of the pulses emitted changes with the amplitude as in the same relation as that before the collapse.<sup>13,14</sup> An example of the increment of

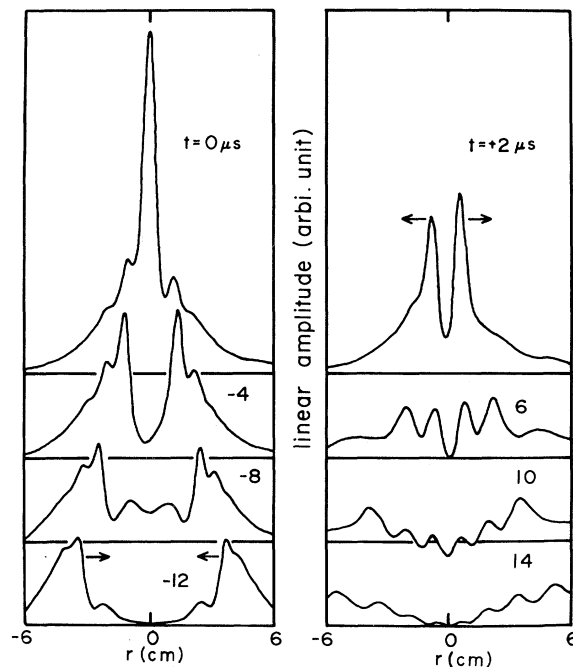


FIG. 2. Spatial evolution of solitons converging to ( $t < 0$ ) and diverging from ( $t > 0$ ) the center ( $t=0$ ) where the collapse of solitons occurs.  $\lambda_D \approx 5.4 \times 10^{-2} \text{ cm}$ .

the number of pulses before and after the collapse are shown in Fig. 3(a), in which the abscissa is taken as the maximum amplitude at the center. When the ingoing soliton exceeds some critical amplitude, the breaking of the soliton occurs. The threshold amplitude measured at the center depends on the electron temperature; higher temperature decreases the threshold values with constant ion temperature, as shown in Fig. 3(b). Third, each pulse produced by the collapse does not show the clear evolution in the wave form, and no more pulses are produced. It is hard to identify all the pulses produced after the collapse but many of their characteristics greatly resemble solitons.

The physical mechanism of scattering is discussed as follows: As the initial amplitude of the excited pulse is getting larger, the nonlinear term takes over the dispersion effects and the initial single pulse breaks into many solitons predicted by Berezin and Karpman<sup>6</sup> or for the periodic initial condition by Zabusky and Kruskal.<sup>5</sup> This condition may be characterized by the pa-

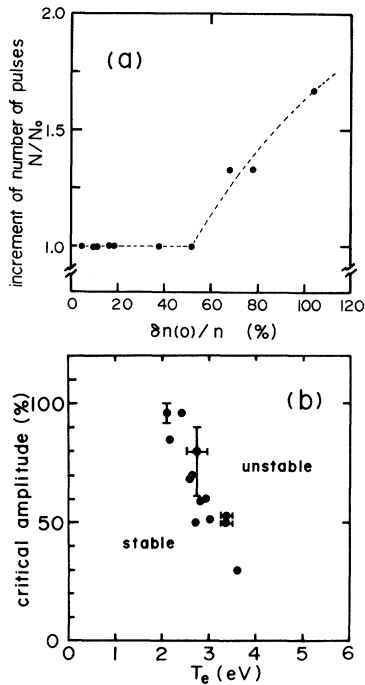


FIG. 3. (a) Increment of number of pulses  $N/N_0$  vs the maximum amplitude  $\delta n(0)/n$  measured at  $r=0$ .  $T_e = 2.9$  eV. (b) Critical amplitude, i.e., the maximum amplitude of the first soliton measured at  $r=0$  vs electron temperature, at the constant ion temperature for the appearance, unstable region, of the second soliton-like pulse.

rameter

$$\sigma \equiv D(U_0/\beta)^{1/2},$$

where  $U_0$  is the initial pulse amplitude,  $\beta = C_s \lambda_D^2 / 2$ ,  $\lambda_D$  is the Debye length, and  $C_s$  is the ion sound velocity. The number of solitons as a function of  $\sigma$  obtained in Ref. 6 are summarized in Fig. 4 with the results obtained in the present experiment. From these results we can confirm that the number of solitons at the center before the collision are well predicted by the theory, but after the collision deviations clearly occur. If we can take the amplitude measured at  $r=0$  as an initial condition, each pulse existing at  $r=0$  with large amplitude should break into many solitons as it travels outward because  $\sigma$ , if we can define it there, ranges between 10 and 15. In the experiment, however, the expected number of pulses has not been observed, but the same number of pulses at the initial position ( $r=0$ ) are observed. Further, the amplitude dependence on radial position after the collapse is also not explained by this manner. Since the characteristics of solitons are only determined by the initial conditions, the result observed after the collapse is hard to understand by the previous theory.

Another possible mechanism is resonant-type scattering of solitons such as the decay instability firstly considered by Newell and Redekopp.<sup>8</sup> This type of scattering appears to be more possible because the phenomenon occurs abruptly near the center and has a threshold value of wave

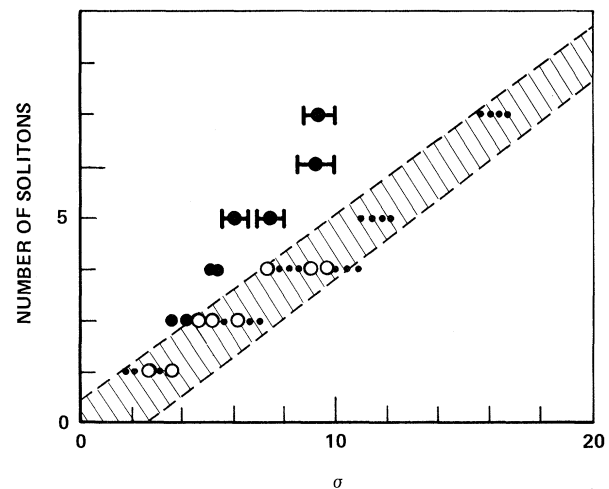


FIG. 4. Number of solitons observed before (open circles) and after (closed circles) the collapse as a function of estimated at  $r=r_0 \approx 3$  cm, for the ingoing pulses. Shaded area and dots are obtained from Ref. 6.

amplitude. Resonant-type scattering process should satisfy the momentum and the energy conservations in the course of the collapse. In the present cylindrical case, we can obtain the resonance condition as follows:

$$\omega_0(k_0) = \sum_{j=1}^N \omega_j(k_j), \quad k_0 = \sum_{j=1}^N k_j, \quad (1)$$

with  $(D_j/\lambda_D)^2 \delta n_j/n$  ( $j=0, 1, \dots, N$ ) being constant as the nature of soliton, where  $\omega_j$  and  $k_j$  are the wave frequency and number of phases of solitons, respectively. The left-hand side of Eq. (1) corresponds to the value before the collapse, and if there are many solitons, all of them should be summed up; the right-hand side corresponds to the state after the collapse.

The experimental results are shown in Fig. 5 by assuming  $\omega = 1/\tau$  and  $k = 1/D$ , where  $\tau$  is the width at half of the full amplitude of soliton in time space. From Fig. 5 we may say that Eq. (1) is satisfied with reasonable agreement. Small deviations are explained as the energy is lost by thermalization of ions at the center where precursor ions are compressed by the wave potential and must be thermalized to heat up the ions,

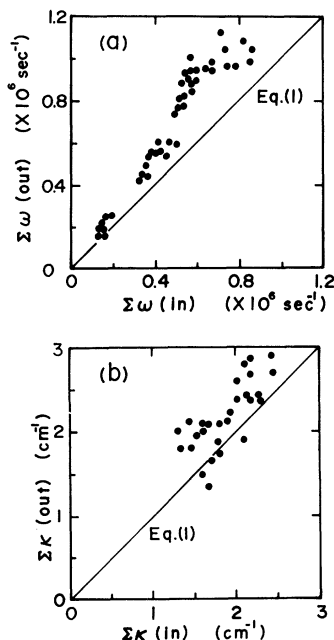


FIG. 5. (a) Energy-conservation relation obtained by changing the wave amplitude.  $\sum\omega(\text{in})$  is the summation of ingoing solitons and  $\sum\omega(\text{out})$  is that of outgoing ones. (b) Momentum-conservation relation obtained in the same condition as in (a).  $\sum k(\text{in})$  is the summation of ingoing solitons and  $\sum k(\text{out})$  is that of outgoing ones.

although the increased ion temperature has not yet been observed. Another confirmation of resonance-type scattering has been seen in that the resonant state may continue for a finite time; the new pulses should have the time delay to be created after the collapse. This phenomenon has been observed in Ref. 14.

When  $T_i$  is finite as in the present case, ion-acoustic pulses with a velocity close to or less than  $C_s$  would be emitted after a main soliton.<sup>15</sup> In the present case, however, pulses produced after the collapse have always larger velocity than  $C_s$ , and are different from ion-acoustic ones.

In conclusion, resonance-type scattering of large-amplitude ion-acoustic cylindrical solitons have been observed experimentally after the collapse at the center of the plasma cylinder. Prior to the collapse, multisoliton phenomena have also been observed to obey theoretical predictions for large-amplitude initial conditions.

The authors are very grateful to Professor Y. Kato, Professor N. Asano, Professor T. Honzawa, and Dr. H. Nakajima for their fruitful discussions and comments. They appreciate the help of Dr. W. A. Peebles for his proof reading and comments. They are also indebted to Mr. S. Fukuda for his assistance in the experiment. This work is supported in part by the Grant-in-Aid for Scientific Research from the Ministry of Education, Japan.

<sup>(a)</sup> Present address: Ashikaga Institute of Technology, Ashikaga, Tochigi Prefecture, Japan.

<sup>1</sup>D. A. Tidman and N. A. Krall, *Shock Waves in Collisionless Plasma* (Wiley, New York, 1971).

<sup>2</sup>V. I. Karpman, *Non-Linear Waves in Dispersive Media*, translated by F. F. Cap (Pergamon, Oxford, England, 1975).

<sup>3</sup>H. Ikezi, R. J. Taylor, and D. R. Baker, *Phys. Rev. Lett.* **25**, 11 (1970).

<sup>4</sup>V. G. Makhankov, to be published.

<sup>5</sup>N. J. Zabusky and M. D. Kruskal, *Phys. Rev. Lett.* **15**, 240 (1965).

<sup>6</sup>Yu. A. Berezin and V. I. Karpman, *Zh. Eksp. Teor. Fiz.* **51**, 1557 (1966) [*Sov. Phys. JETP* **24**, 1049 (1967)]; Yu. A. Berezin, *Zh. Tekh. Fiz.* **38**, 24 (1968) [*Sov. Phys. Tech. Phys.* **13**, 16 (1968)].

<sup>7</sup>N. Hershkovitz, T. Romesser, and D. Montgomery, *Phys. Rev. Lett.* **29**, 1586 (1972).

<sup>8</sup>A. C. Newell and L. G. Redekopp, *Phys. Rev. Lett.* **38**, 377 (1977).

<sup>9</sup>S. Maxion and J. Viecelli, *Phys. Fluids* **17**, 1614 (1974).

<sup>10</sup>T. Ogino and S. Takeda, *J. Phys. Soc. Jpn.* **41**, 257 (1976).

<sup>11</sup>T. Chen and L. Schott, *Plasma Phys.* **19**, 959 (1977).

<sup>12</sup>S. Maxion and J. Viecelli, *Phys. Rev. Lett.* **32**, 4 (1974).

<sup>13</sup>N. Hershkowitz and T. Romesser, *Phys. Rev. Lett.* **32**, 581 (1974).

<sup>14</sup>Y. Nishida, T. Nagasawa, and S. Kawamata, *Phys. Lett.* **69A**, 196 (1978).

<sup>15</sup>P. H. Sakanaka, *Phys. Fluids* **15**, 304 (1972).

## Metallic Xenon at Static Pressures

David A. Nelson, Jr., and Arthur L. Ruoff

*Department of Materials Science and Engineering, Cornell University, Ithaca, New York 14853*

(Received 27 September 1978)

Using a diamond indenter, diamond anvil technique along with nonshorting interdigitated electrodes produced on the anvil by lithographic processes, we have shown that the electrical resistance of a xenon sample at 32°K drops from  $10^{13} \Omega$  (or greater) to about  $10^4 \Omega$  at 0.33 Mbar. Further studies using a second method reveal that the resistivity has dropped to below  $10^{-1} \Omega \text{ cm}$  and possibly much lower.

The present paper demonstrates the production of a conducting state in xenon which is produced by the application of high pressure on a solid sample of xenon at 32°K. The experimental techniques are described first. Then there is a brief discussion of why xenon is expected to become metallic at high pressures.

When a spherical diamond tip of radius  $R$  is pressed against a flat diamond, a contact pressure is established. The pressure distribution can be accurately calculated by the Hertz contact theory,<sup>1</sup> from a knowledge of the tip radius  $R$ , the applied force  $F$ , Young's modulus  $E$ , and Poisson's ratio  $\nu$ .<sup>2,3</sup> The fact that diamond is nearly isotropic elastically, and hence can be represented by an isotropic elastic solid, has been described elsewhere.<sup>3</sup> If  $a$  is the radius of the contact circle and  $r$  is a variable radius, then the pressure distribution is given by

$$P = P_0(1 - a^2/r^2)^{1/2}, \quad (1)$$

where

$$P_0 = \left(\frac{3}{2}\right)^{1/3} \pi^{-1} [E/(1 - \nu^2)]^{2/3} R^{-2/3} F^{1/3}. \quad (2)$$

We use  $E = 1141 \text{ GPa}$  and  $\nu = 0.07$ .<sup>3</sup> For diamond at 50 GPa, the pressure computed from Hertz contact theory agrees with the directly measured value obtained by the use of Newton's-ring techniques.<sup>3,4</sup> Ruoff and Wanagel have used this indenter-anvil technique to obtain pressures of 1.4 Mbar.<sup>2</sup>

Measurements of insulator-to-metal transitions can be made using the interdigitated-electrode technique developed by Ruoff and Chan.<sup>5</sup> A schematic drawing of this electrode system is shown in Fig. 1. The actual electrodes involve

75 or more fingers. They are produced by photolithography although electrodes with smaller finger widths and smaller spacing can be produced by electron-beam lithography. The value of  $d$  in the present experiments is  $3 \mu\text{m}$ . The electrodes used in these experiments are nickel, deposited by sputtering; they are  $350 \text{ \AA}$  thick. Electrical leads are attached to the anvil base. Then the sample is deposited on the anvil. Finally, the indenter is pressed against the sample-electrode-anvil assembly resulting in contact over the region shown by the dashed circle in Fig. 1. When the pressure near the center reaches a sufficiently high value, the sample undergoes an insulator-to-metal transition and the electrode circuit is closed. The metallic region is represented by a solid circle in Fig. 1 for two different cases of indenter location. The center pressure will be different for these two cases when the transition is observed; by making the finger widths and spacings sufficiently small, the pressure at which the transition is observed will approach the center pressure. The technique used with ZnS led to a transition pressure<sup>5</sup> of  $14.0 \pm 0.5 \text{ GPa}$ ; this transition is observed at  $15.0 \pm 0.5 \text{ GPa}$  on the ruby scale.<sup>6</sup>

In the present experiment the anvil (with its interdigitated electrodes) is placed in a vacuum chamber. Following evacuation, the anvil, which rests on a plate through which helium can flow, is cooled to 32°K. The temperature is measured with a platinum resistance thermometer. Xenon is then introduced into the chamber and condenses on the anvil. The thickness of the xenon is measured by a quartz thickness monitor, the quartz crystal being located adjacent to the dia-

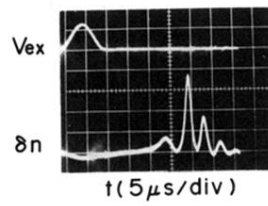


FIG. 1. Example of the applied pulse (top trace) and excited solitons observed at the column center (bottom trace).